JOURNAL OF MAGNETIC RESONANCE 64, 81–93 (1985)

Stimulated Echo Imaging

J. FRAHM, K. D. MERBOLDT, W. HÄNICKE, AND A. HAASE

Max-Planck-Institut für biophysikalische Chemie, Postfach 2841, D-3400 Göttingen, Federal Republic of Germany

Received March 11, 1985

A new form of NMR imaging is described using stimulated echoes. The technique, dubbed STEAM (*st*imulated *e*cho *a*cquisition *m*ode) imaging, turns out to become a versatile tool for multipurpose NMR imaging. Stimulated echoes can be excited by a sequence of at least three rf pulses, which in the basic experiment have flip angles of 90° or less. Thus no selective or nonselective 180° pulses are needed, which eliminates a variety of problems associated with such pulses in conventional spin-echo NMR imaging. Further advantages of STEAM imaging are concerned with the functional flexibility of an imaging sequence comprising three pulses and three intervals and the possibility of "storing" information prepared during the first interval into the form of longitudinal magnetization during the second interval. In general, the applied rf power is considerably reduced as compared to spin-echo-based imaging sequences. Here the general principles of the technique are outlined and first applications to multislice imaging of directly neighboring slices are demonstrated. Subsequent papers will be concerned with modifications of the basic STEAM sequence which, for example, allow multiple chemical-shift-selective (CHESS) imaging, complete imaging of the spin–lattice relaxation behavior, diffusion imaging, and single-shot real-time imaging.

INTRODUCTION

Except for the very first attempts involving free induction decays, NMR imaging has been based on the acquisition of spin-echo (SE) NMR signals excited by rf pulse sequences of the form $90°–(180°–SE–)_n$. These sequences provide the maximum signal available for reconstruction of an image and yield excellent anatomical and diagnostic details. Nevertheless, NMR experiments including 180° pulses are limited in various respects in particular when applied to the imaging of living subjects.

(i) The use of selective 180° pulses in combination with a slice selection gradient raises problems for proper refocusing of the excited spin moments, see, e.g., (*1*). A solution requires increase of the bandwidth of the 180° pulse but distorts magnetization immediately on both sides of the wanted slice. Moreover, in most cases a second "compensation" experiment is needed to eliminate magnetization components contributing from outside the slice. The first effect degrades the use of multislice imaging, while the second effect prolongs the measuring time by a factor of two.

(ii) SE-NMR sequences are entirely based on transverse magnetization which can be excited once and then must be used in a time short with respect to T_2 under the assumption of multiecho formation by means of a sequence of 180° pulses. For a more quantitative imaging, it is a disadvantage that the attenuation of the spin

0022-2364/85 $3.00

echoes results from a variety of processes which together destroy the phase coherence of the spin moments. *In vivo* the simultaneous presence of T_2 relaxation, diffusion, and flow makes a clear separation or discrimination of contributions almost impossible. Further, since no longitudinal magnetization is involved, spin echoes do not contain any T_1 information. In SE-NMR imaging, therefore, "T_1 contrast" has to be acquired in a rather time-consuming way by performing multiple imaging experiments with different repetition times or by means of recording multiple inversion–recovery images with different relaxation delays.

(iii) To provide a maximum of information within the measuring time of a single NMR image, SE techniques have been extended to multiecho and/or multislice versions using a large number of 180° pulses. These sequences, however, become a problem in high-field NMR imaging at field strengths of 1.5 T or higher because of the considerable increase of the rf power dissipation in the human body. A reduction of SE-NMR sequences to the safety guidelines in most cases might preclude a truly economic use of appropriate imaging systems.

Here we will present a new form of NMR imaging using stimulated echoes which is free from the above-mentioned drawbacks simply by avoiding the application of 180° pulses. Although the stimulated echo intensity is only half that of a spin echo taken at the same readout time (i.e., the time corresponding to the first and third intervals of the three-pulse sequence, see below), the advantages of STEAM imaging and some of its modified versions will definitely compensate for this partial loss in signal-to-noise. It is our belief that new pulse sequences which reduce the measuring times, which give access to new or more accurate information, and which thus provide improved specificity rather than optimized signal-to-noise, will become increasingly important in future applications of NMR imaging. In fact, STEAM imaging experiments will be described which often are without SE-NMR alternatives including simultaneous chemical-shift-selective (CHESS) imaging of multiline spectra (*2*), simultaneous imaging of complete spin–lattice relaxation curves (*3*), imaging of self-diffusion coefficients (*4*), and single-shot real-time imaging with a variable spatial resolution (*5*).

STIMULATED ECHOES

The basic rf pulse sequence that gives rise to a stimulated echo (STE) signal at $t_3 = t_1$ is

$$90°\text{–}t_1\text{–}90°\text{–}t_2\text{–}90°\text{–}t_3(\text{STE}) \qquad [1]$$

where the pulses may have arbitrary phase relations. It was first described by Hahn in 1950 (*6*) and was later used for NMR diffusion measurements (*7, 8*). More recently, STE signals have been observed with certain two-dimensional and multiple-quantum NMR experiments. Figure 1 depicts an experimental demonstration of the signals excited by sequence [1] in the presence of a magnetic field gradient. In general, five echoes may be observed by application of three pulses. Assuming $t_2 > t_1$ the primary echo signals are the SE signal at $t_2 = t_1$ created by the first two pulses and the STE signal at $t_3 = t_1$ which is due to the action of all three pulses. Secondary echoes occur as spin echoes excited by the third pulse which mirrors the primary SE signal to yield a second SE at $t_3 = t_2 - t_1$, the FID following the second

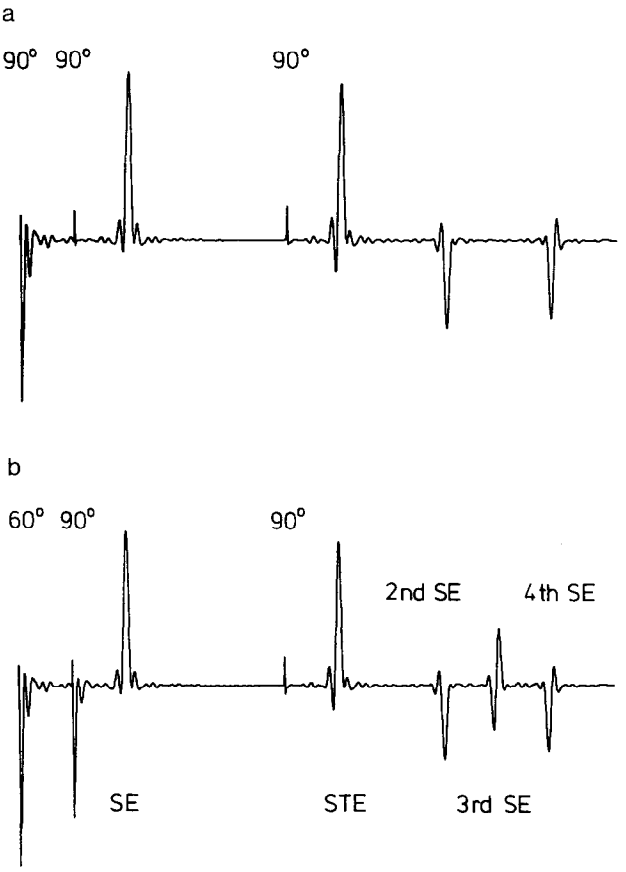

FIG. 1. Experimental demonstration of NMR signals excited by a sequence of three nonselective rf pulses in the presence of a gradient. SE, spin echo; STE, stimulated echo; 2nd SE, spin echo of the initial spin echo; 3rd SE, spin echo of the FID following the second pulse; and 4th SE, spin echo of the FID following the first pulse. (a) 90°–90°–90° pulse sequence. (b) 60°–90°–90° pulse sequence.

pulse to yield a third SE at $t_3 = t_2$, and the FID following the first pulse to yield a fourth SE at $t_3 = t_1 + t_2$. The third SE signal is seen only in Fig. 1b, where longitudinal magnetization has been left by the initial 60° pulse for excitation by the second pulse. Without an FID after the second pulse the corresponding spin echo after the third pulse is missing as demonstrated in Fig. 1a.

Transverse magnetizations following the initial 90°(x') pulse acquire phase information while precessing during the first interval of length t_1. At the time of a second 90°(x') pulse only those vector components that are aligned along the y' axis in the rotating frame of reference are transformed into (phase-encoded) longitudinal magnetizations. Assuming an equal distribution of transverse components within the x', y' plane prior to the second pulse, the affected $M_{y'}$ components represent half of the total magnetization and give rise to a stimulated echo at $t_3 = t_1$ after application of a third ("read") pulse. The remaining half of the total

magnetization, i.e., the $M_{x'}$ components, refocus at $t_2 = t_1$ to form a conventional spin echo. Phase information may be related to spin–spin couplings or resonance offsets, i.e., chemical shifts in an NMR spectrum or a distribution of spatially encoded frequencies due to magnet inhomogeneities or deliberate applications of magnetic field gradients. In fact, the experimental conditions encountered in 1950 by Hahn directly corresponded to the situation in current state NMR imaging where homogeneous magnets are combined with magnetic field gradients of the order of 1 to 10 mT m^{-1}.

Another important feature of sequence [1] is that the flip angles may be reduced without much loss in intensity of the primary SE and STE signals. The effect is clearly demonstrated in Fig. 2 where the flip angles of the second and third pulses are varied from 90 to 10°, respectively. Experimentally, a 10° pulse in the third position still gave a signal intensity of almost 20% of the 90° result. If both the second and third pulses are reduced to 60° (45°), the corresponding STE amplitude is attenuated to about 85% (60%) with respect to that obtained by a 90° pulse. A variation of the flip angle of the first pulse parallels the well-known findings for the intensity of the conventional FID signal. On the other hand, a single 180° pulse in any of the three positions eliminates the stimulated echo.

In general, not only the STE but all signals resulting from application of a three-pulse sequence may be exploited for NMR imaging. At least the primary spin echo is well suited for imaging purposes and will be used in many STEAM imaging techniques in addition to the stimulated echo. In fact, the SE and STE signals may even be added to regain the same signal intensity as obtained with a conventional SE-NMR sequence, although it is often just the different use of both images that may increase the information available from a single STEAM imaging experiment. The outstanding properties, however, which make STE signals particularly attractive for NMR imaging, are due to (i) the "storage" effect of the intermediate interval t_2, where the phase-encoded magnetization relaxes rather slowly with the spin–lattice relaxation time T_1, so that phase information can be conserved for a long period and then be refocused as a STE signal; (ii) the possibility of a successive partial readout of STE signals by means of a series of "third" pulses which may be slice selective or chemical-shift selective or which may have small flip angles; and (iii) the possibility of discriminating between phase-encoded longitudinal magnetizations yielding a STE signal and normal (random) longitudinal magnetizations resulting in an FID after application of a third pulse. The storage, the portioning, and the compartmentation of phase-encoded ("prepared") magnetization offer a variety of ways for the design of improved or entirely new NMR imaging experiments to be discussed below as well as in subsequent papers.

BASIC SEQUENCES FOR NMR IMAGING USING STIMULATED ECHOES

Some basic pulse and gradient sequences for NMR imaging using stimulated echoes are shown in Fig. 3. In their most simple form STEAM sequences contain only a single slice-selective (90°) pulse and give rise to the observation of a single stimulated echo. The corresponding sequences shown in Figs. 3a–c demonstrate the great functional flexibility of the pulses as well as the variability of the gradient switches. Frequency-selective pulses of arbitrary pulse shapes are represented by rf

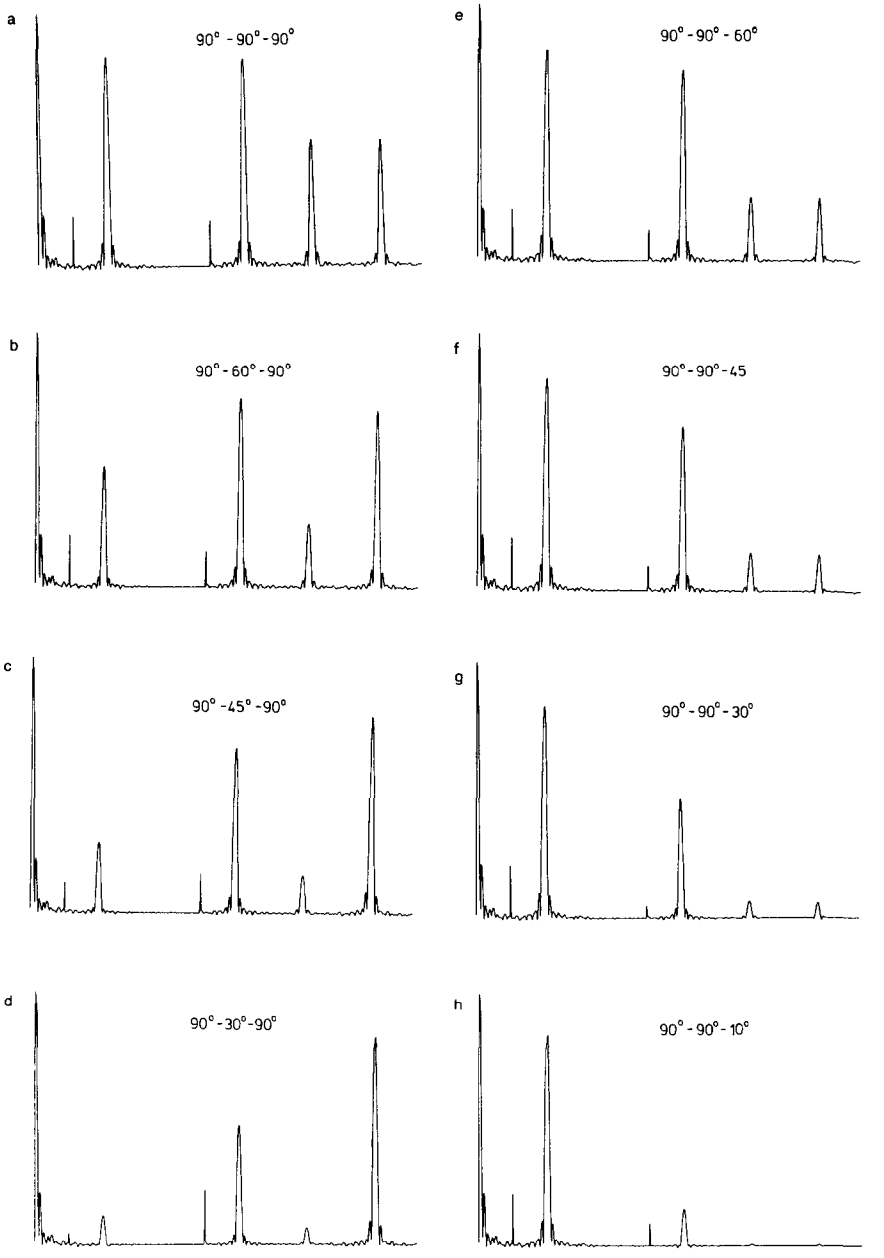

FIG. 2. Flip-angle dependence of echo signals excited by a sequence of three nonselective rf pulses in the presence of a gradient. Amplitudes correspond to magnitude values. (a) 90°–90°–90° pulse sequence. (b–d) Three-pulse sequence with flip angles of 60, 45, and 30° for the second pulse, respectively. (e–h) Three-pulse sequence with flip angles of 60, 45, 30, and 10° for the third pulse, respectively.

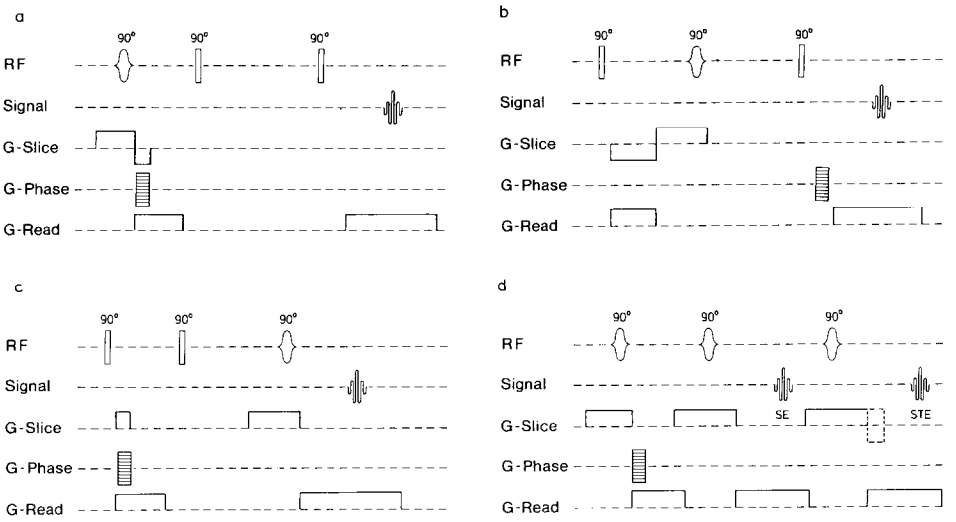

FIG. 3. Schematic diagrams of basic STEAM imaging sequences. (a–c) Sequences using a single slice-selective rf pulse in the first, second, or third position, respectively. (d) Sequence using three slice-selective rf pulses. Broken lines indicate refocusing parts of the slice gradient which are self-compensating and thus may be omitted.

pulses with a Gaussian pulse shape. They may be chemical-selective pulses or, in combination with a gradient, slice selective or so-called zoom pulses. Nonselective pulses of arbitrary shapes are represented by pulses with rectangular pulse shapes and are defined by the fact that their application excites the entire NMR spectrum. In many cases nonselective pulses may be advantageously replaced by frequency-selective pulses of various functions.

The three intervals of the STEAM sequence may be used to minimize situations in which different gradients have to be switched simultaneously. For example, proper refocusing of the slice-selection gradient may take place immediately after or before application of the respective rf pulse by inversion (compare Figs. 3a, b), or by using a defocusing gradient of the same sign in the first interval (compare Fig. 3c). It is worth noting that the diagrams shown in Figs. 3b, c represent new gradient schemes not applicable with SE-NMR imaging sequences because defocusing gradients are applied prior to the combined use of the slice-selection pulse and gradient. Figure 3d gives an example for a STEAM sequence comprising three slice-selective pulses with the simultaneous observation of the primary SE and STE signals. As is demonstrated by the broken lines, some parts of the various refocusing gradients may become self-compensating thereby simplifying the resulting gradient sequence.

As already indicated by the scheme shown in Fig. 3d slice-selective rf pulses within STEAM imaging sequences may be arbitrarily combined even independent of the directions of the gradients. Furthermore slice-selective pulses may have an identical length/bandwidth as is demonstrated by computer simulations shown in Figs. 4a–d. The diagrams refer to magnetization profiles as obtained by a numerical

solution of the Bloch equations for slice selection by some typical STEAM imaging experiments. For details of the calculations see Ref. (*1*). The profiles of interest correspond to the $M_{y'}$ components of the transverse magnetization (solid lines). For comparison with the STEAM sequences, Fig. 4a depicts the case of a single slice-selective 90°(x') pulse with a Hamming pulse shape and refocusing by inversion of the gradient. Figures 4b, c contain pulse and gradient sequences with the slice-selective pulse in the third and second positions, respectively, while Fig. 4d shows the combination of two slice-selective pulses of identical length. In all cases similar slice profiles could have been obtained without inducing distortions of magnetizations close to the excited slice and thus without the need for a second "compensating" experiment.

The phase-encoding gradient as well as the read gradients are used in the same way as for conventional SE-NMR imaging. However, the position of the phase-encoding gradient within the STEAM sequence will select its action on the SE and/or STE signals. If applied in the first interval as demonstrated in Fig. 3d, then both the SE and STE signals are similarily affected. In contrast, an application after the second pulse will affect only the SE signal, while an application after the third pulse will affect only the STE signal. Thus it becomes possible to use different phase-encoding gradients for independent imaging with the SE or STE signals, respectively. Appropriate experiments may be concerned with the simultaneous imaging of a plane with normal gradients and with magnified gradients producing a so-called zoom image. Such a technique is demonstrated in the pulse and gradient scheme shown in Fig. 5a. Another example may be the use of two different phase-encoding gradients for encoding spatial and flow information separately into the SE and STE signals.

MULTISLICE IMAGING USING STIMULATED ECHOES

Conventional multislice imaging techniques rely on repetitions of the entire pulse and gradient sequence with different irradiation frequencies. Although multislice SE-NMR imaging may be performed as a time-sharing experiment, the time needed for a single slice is of the order of 100 ms which leads to the recording of 10 slices with repetition times of about 1 to 1.5 s. STEAM imaging sequences provide a very efficient alternative: a general scheme for multislice imaging even of arbitrarily spaced slices is shown in Fig. 5b. The entire imaging volume is prepared by two

FIG. 4. Plane selection in STEAM imaging using selective 90°(x') pulses (Hamming profile) in combination with a z gradient of strength 10 mT m^{-1}. The pulse and gradient sequences are symbolically indicated at the top of each figure. The durations of the intervals t_1 and t_2 are of the order of 10 to 30 ms depending on the gradients which have to be applied within a complete imaging sequence. In the lower parts, computer-simulated magnetization profiles are shown which display the magnetizations M_z (dotted line), $M_{x'}$ (dashed line), and the observed magnetization $M_{y'}$ (solid line) as a function of the spatial coordinate z. The equilibrium magnetization M_0 is normalized to one. Relaxation effects (T_1 = 1 s, T_2 = 0.05 s) are included. (a) Application of a single selective 90° pulse with proper refocusing of the gradient. (b) STEAM imaging sequence with a single selective 90° pulse in the third position. (c) STEAM imaging sequence with a single selective 90° pulse in the second position using defocusing prior to application of the rf pulse. (d) STEAM imaging sequence with two selective 90° pulses of identical length (i.e., identical bandwidth) in the first and third positions.

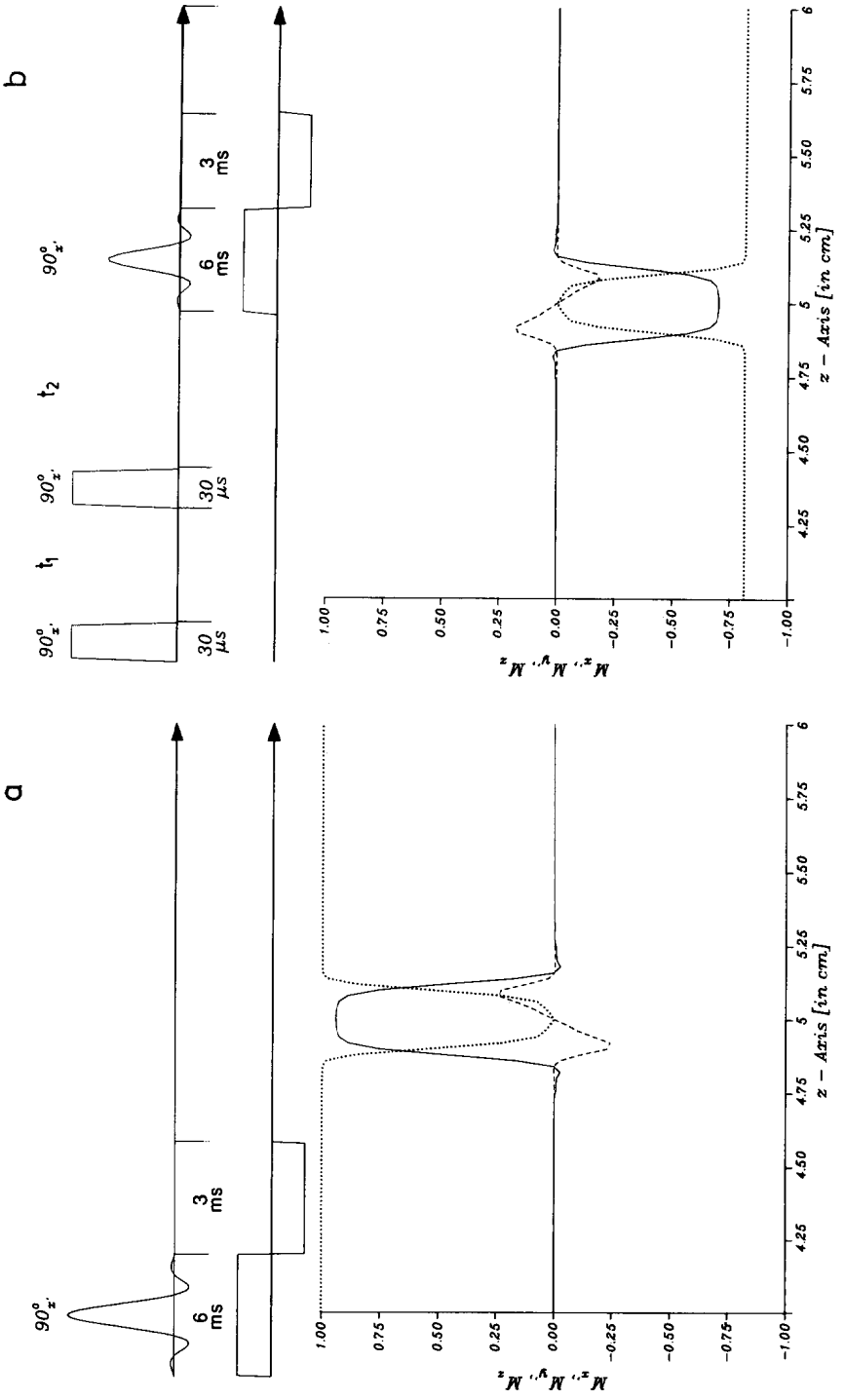
a
b
90°_x
t_1
90°_x
t_2
90°_x
6 ms
3 ms
30 μs
30 μs
6 ms
3 ms
M_z, M_y, M_z
z – Axis [in cm]
1.00
0.75
0.50
0.25
0.00
−0.25
−0.50
−0.75
−1.00
4.25
4.50
4.75
5
5.25
5.50
5.75
6

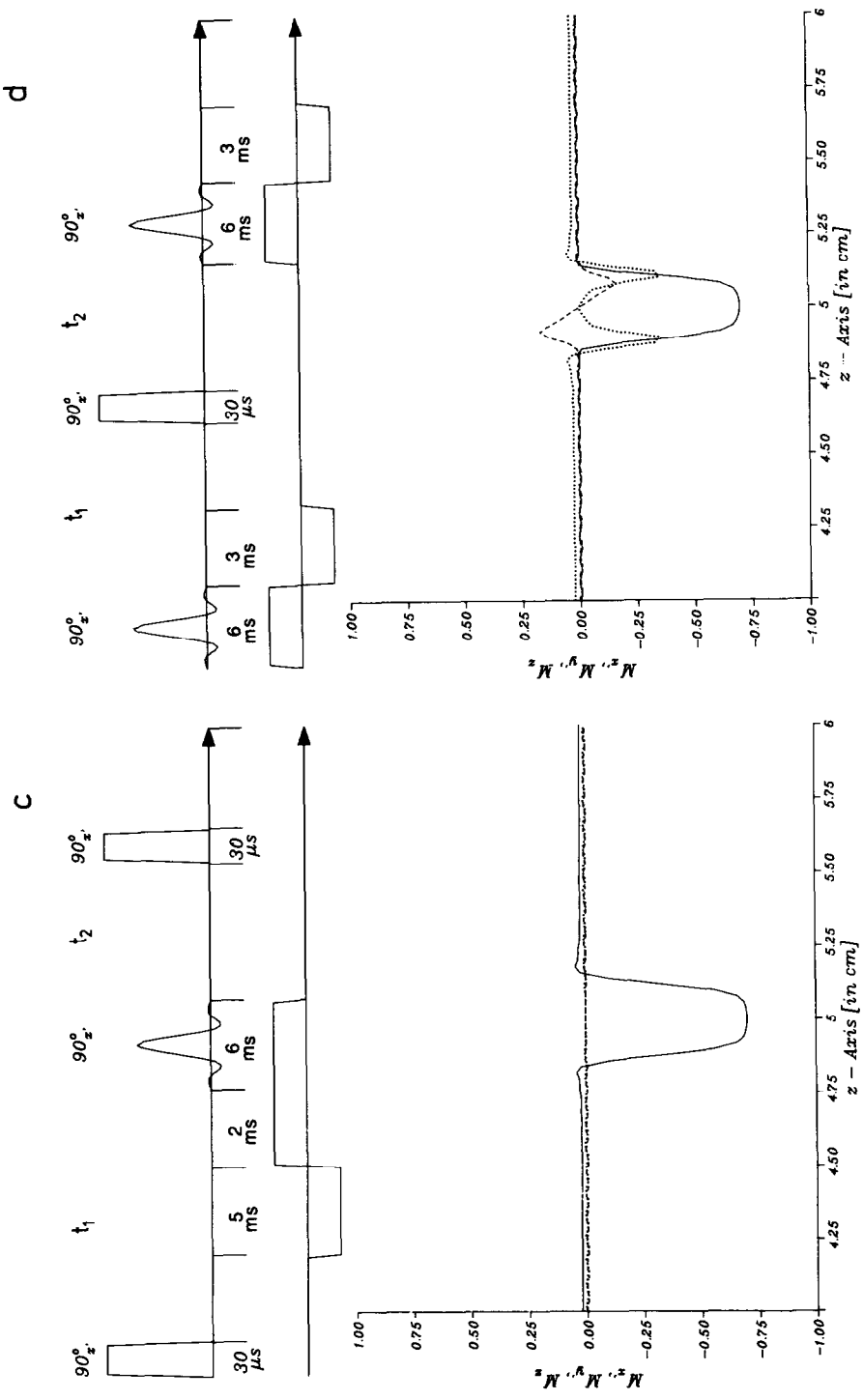
d
90°x'
t1
90°x'
t2
90°x'
6 ms
3 ms
30 μs
3 ms
6 ms
1.00
0.75
0.50
0.25
0.00
−0.25
−0.50
−0.75
−1.00
Mx', My', Mz
4.25
4.50
4.75
5
5.25
5.50
5.75
6
z – Axis [in cm]
c
90°x'
t1
90°x'
t2
90°x'
30 μs
5 ms
2 ms
6 ms
30 μs
1.00
0.75
0.50
0.25
0.00
−0.25
−0.50
−0.75
−1.00
Mx', My', Mz
4.25
4.50
4.75
5
5.25
5.50
5.75
6
z – Axis [in cm]

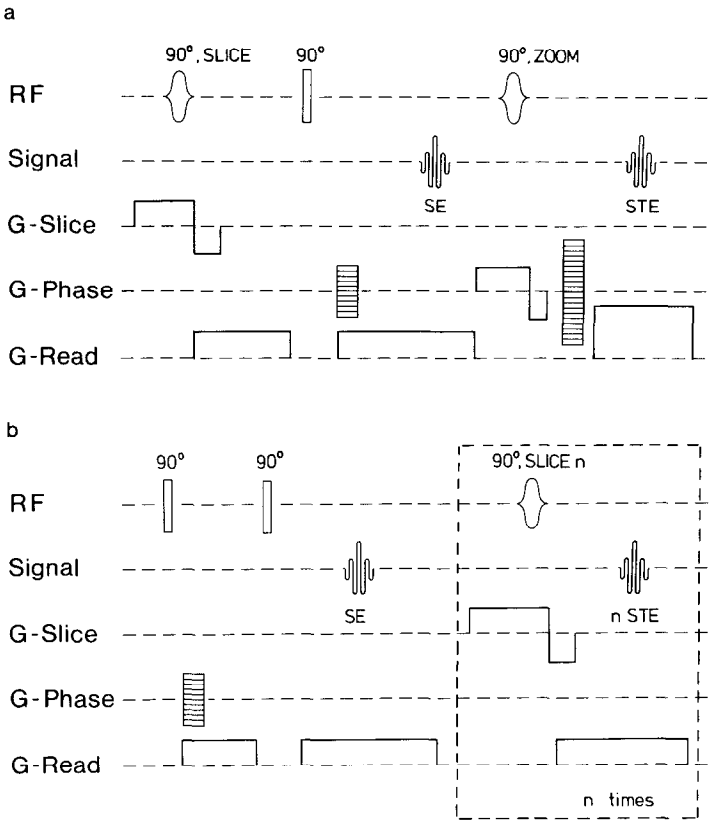

FIG. 5. Schematic diagrams of STEAM imaging sequences. (a) Simultaneous acquisition of an overview and zoom image using the SE and STE signals, respectively. (b) Multislice imaging using stimulated echoes.

leading nonselective rf pulses. They give rise to a SE signal in the second interval which, if wanted, may be used to create a so-called "transmission" image without slice selection. The final part of the sequence performs the slice selection and the acquisition of the corresponding STE signal. Only this part is repeated n times to create n cross-sectional images out of the entire excited volume. It should be noted that the irradiation frequency is selected prior to application of the slice selective pulses and is reset immediately after its termination to enable data readout with respect to the normal frequency, i.e., spatial position. The time needed for a single slice is of the order of 20 to 30 ms; the rf power corresponds to a single 90° pulse. Subsequent readout of different slices becomes possible due to the property of the STEAM imaging sequences of "storing" magnetization prepared by the first two pulses into longitudinal magnetization which then decreases rather slowly with T_1. Slice-selective "third" pulses induce only STE signals which belong to magnetization of the corresponding frequency interval. All other magnetization is unaffected and remains "stored."

The major advantages of multislice STEAM imaging are threefold: low rf power and reduced gradient switching, reduced measuring times or increased number of slices, and the benefit of avoiding 180° pulses which allows one to image directly

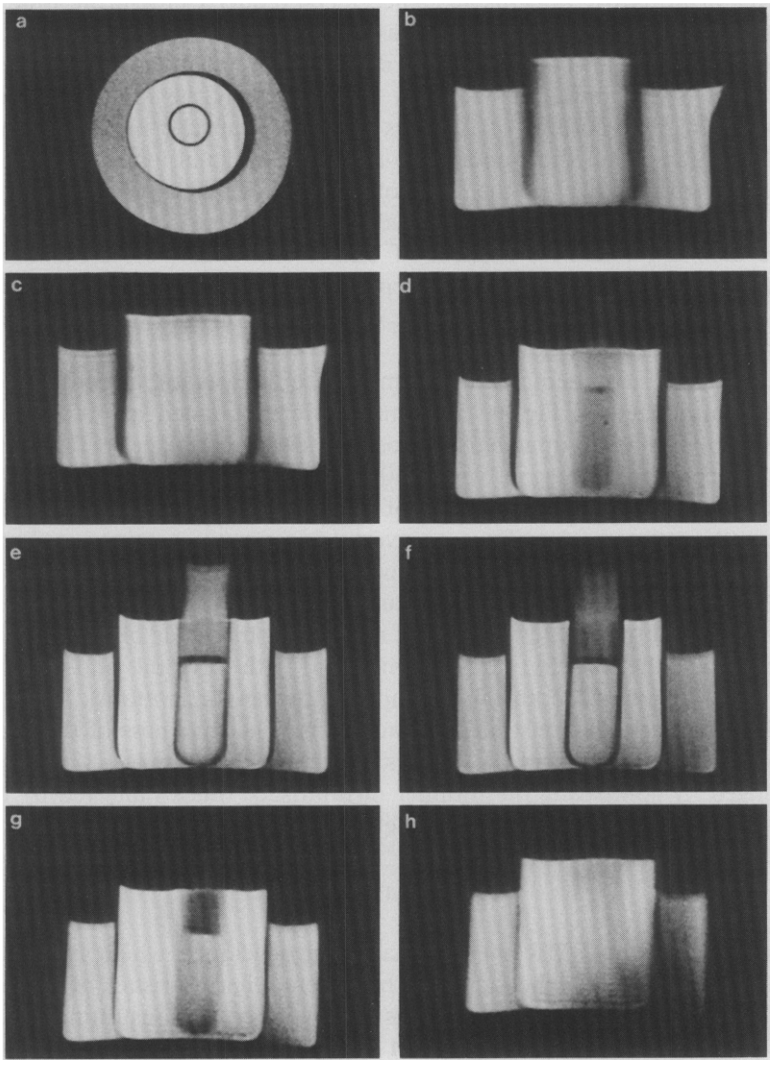

FIG. 6. 100 MHz (2.3 T) ^{1}H NMR images of a cylindrical phantom (72 mm diam) filled with olive oil containing a bottle (40 mm diam) of water and another tube (10 mm diam) filled with both water (on bottom) and oil (on top). All images are "raw" images which have not been subjected to a smoothing or filtering procedure. (a) Image of a horizontal slice of thickness 4 mm. (b–h) Transaxial multislice STEAM images of directly neighboring slices (spacing 4 mm, thickness 4 mm) selected out of a series of 10 images. Although the entire acquisition time, i.e., the time needed for recording a single set of "projections' of all 10 slices, was only 250 ms, the repetition time has been set to 1 s due to limitations of our present computer facilities.

neighboring slices. If desired, slice distances, slice thicknesses, and image sizes may be varied from slice to slice within the sequence. It should be emphasized that multislice STEAM imaging provides a solution to the problem of economic imaging in high magnetic fields where rf power absorption becomes a problem for multiple applications of SE-NMR imaging sequences. The reduced measuring time per slice improves the imaging efficiency insofar as faster repetition times become possible. Actual limitations might be due to slow data transfer rates and/or small computer memory sizes. NMR limitations are only determined by the spin–lattice relaxation times. However, the recording of 16 slices typically requires a measuring interval of about 0.4 s which is still short enough to account for signal losses because of water proton relaxation with a T_1 of the order of 1 s or higher in magnetic fields of about 2 T. On the other hand, a region scanned by 16 neighboring slices corresponds to a volume of 8 cm thickness if slices of only 5 mm thickness are chosen. Since proper computer equipment will allow repetition times of about 0.5 s for the above example, a set of 16 (overview) images, each based on 128 different projections, may be recorded in about 1 min.

Experimental results demonstrating multislice images of directly neighboring slices are summarized in Fig. 6. The images were obtained at 100 MHz proton NMR frequency using an imaging/spectroscopy system (Bruker BNT 100) based on a 2.3 T superconducting magnet with a 40 cm bore. The measuring time was about 4 min corresponding to the recording of 256 different phase-encoded projections with a repetition time of 1 s. Thus no averaging or compensation experiment was employed. The SE transmission image is not shown. Instead, Fig. 6a displays a cross-sectional slice perpendicular to the multislice images to illustrate the arrangement of the three concentric bottles: the outer one (inner diameter of 72 mm) has been filled with water, the middle one (40 mm diam) with olive oil, and the inner one (10 mm diam) contained both oil (on top) and water (on bottom). The chemical-shift artifact is clearly demonstrated in this plane. The thickness of the slices in all cases as well as the distance of the centers of the multislice images was 4 mm. This can be judged by comparing the number of multislice images affected by the inner tube (i.e., Figs. 6d–g) with Fig. 6a and the tube diameter of 10 mm.

CONCLUSIONS

A new principle for NMR imaging has been developed which is based on the acquisition of stimulated echo signals. The general characteristics of the technique are described and first experimental results are presented demonstrating an improved method for multislice imaging. STEAM imaging arises as a versatile tool for a variety of applications in NMR imaging. General advantages are concerned with improvements in security by reducing the applied rf power, in efficacy of imaging investigations by increasing the quality and quantity of information per time, and in parametric resolution as will be described in subsequent papers on chemical-shift-selective imaging, T_1 imaging, and diffusion imaging. Stimulated echo imaging will arise as a new tool for multipurpose investigations leading to a considerable gain in accuracy and specificity in NMR imaging.

ACKNOWLEDGMENTS

This work has been supported by the Bundesminister für Forschung und Technologie (BMFT) of the Federal Republic of Germany (Grant 01 VF 242). Computer simulations were performed using the facilities of the Gesellschaft für Wissenschaftliche Datenverarbeitung Göttingen (NAG software).

REFERENCES

1. J. FRAHM AND W. HÄNICKE, *J. Magn. Reson.* **60,** 320 (1984).
2. A. HAASE AND J. FRAHM, *J. Magn. Reson.* **64,** 94–102 (1985).
3. A. HAASE AND J. FRAHM, *J. Magn. Reson.*, in press.
4. K. D. MERBOLDT, W. HÄNICKE, AND J. FRAHM, *J. Magn. Reson.*, in press.
5. J. FRAHM, A. HAASE, D. MATTHAEI, K. D. MERBOLDT, AND W. HÄNICKE, *J. Magn. Reson.*, in press.
6. E. L. HAHN, *Phys. Rev.* **80,** 580 (1950).
7. D. E. WOESSNER, *J. Chem. Phys.* **34,** 2057 (1961).
8. J. E. TANNER, *J. Chem. Phys.* **52,** 2523 (1970).